Observation of the freezing line in a deuteron glass

Z. Kutnjak,* R. Pirc, A. Levstik, I. Levstik, C. Filipič, and R. Blinc
Jožef Stefan Institute, 61111 Ljubljana, Slovenia

R. Kind
Eidgenössische Technische Hochschule Zürich–Hönggerberg, Institut für Quantenelektronik, 8093 Zürich, Switzerland

(Received 15 July 1994)

The phase diagram of the deuteron glass $Rb_{1-x}(ND_4)_xD_2PO_4$ has been determined experimentally in the entire range of concentration x. A recently introduced temperature-frequency plot has been used to analyze the shape of the dielectric relaxation spectrum, indicating that in the glassy regime the longest relaxation time diverges according to the Vogel-Fulcher law. The corresponding Vogel-Fulcher temperature has been identified as the static limit of the freezing temperature T_f. The phase boundaries of the ferroelectric and antiferroelectric phases have been obtained in a standard manner by observing the peaks and breaks, respectively, in the temperature dependence of the quasistatic dielectric constant. It is shown that in a broad concentration range the observed phase diagram can be quantitatively described by a mean-field theory based on the static random-bond random-field model of dipolar glasses. The absence of macroscopic polarization in the ferroelectric region close to the glassy phase is probably due to the formation of microdomains in the presence of local random fields, however, recent NMR data suggest that a phase segregation between ferroelectric and glassy regions may occur.

I. INTRODUCTION

The dynamics of the freezing transition in spin glasses and their electric analogues, namely, proton and deuteron glasses, has remained one of the central problems in condensed matter physics. In the latter category, the mixed ferroelectric-antiferroelectric solid solution $Rb_{1-x}(ND_4)_xD_2PO_4$ (abbreviated as DRADP-x) has probably been investigated more thoroughly than any other glassy system,[1,2] however, its (x,T) phase diagram is still not completely understood. The main difficulty is—like in any other glassy system—the extreme slowing down of the relaxation process on approaching the freezing temperature T_f, which is furthermore characterized by many time scales.[3,4] Typically, the observed splitting between the field-cooled and zero-field-cooled dielectric constants yields a value for T_f which depends on the experimental time scale $t_{\rm expt}$, i.e., $T_f = T_f(t_{\rm expt})$.[5] Thus a static value of T_f is not directly accessible and could only be obtained by the appropriate extrapolation to infinite observation times, namely, $T_f = T_f(t_{\rm expt} \to \infty)$. This, in turn, calls for better understanding of the relaxation process itself which might be gained by means of a dynamic experiment such as the measurement of the complex dielectric constant $\varepsilon^*(\omega) = \varepsilon'(\omega) - i\varepsilon''(\omega)$ in a broad range of frequencies ω.

A common method to determine T_f from the dielectric data is based on the observation that both $\varepsilon'(\omega,T)$ and $\varepsilon''(\omega,T)$ show a maximum as functions of temperature. For example, the temperature $T_{\rm max}(\omega)$ at which the maximum of one of these occurs has been found empirically[6] to scale with ω according to the Vogel-Fulcher (VF) relation

$$\omega = \omega_0 \exp[-E/(T_{\rm max} - T_0)] , \qquad (1)$$

where ω_0, E, and T_0 are parameters of the system. One is obviously tempted to interpret T_0 as the static limit of the freezing temperature T_f, however, there will be in general two different sets of parameters for the real and imaginary parts of the dielectric constant and thus the choice of T_f is not unique. Besides, the physical background of Eq. (1) remains unclear.

In a similar approach, one adopts a relation of the type (1) for the relaxation frequency $f = 1/\tau$, where τ is the relaxation time. The underlying general idea is that the complex dielectric constant can be written as a sum of Debye relaxations,

$$\varepsilon^*(\omega) - \varepsilon_\infty = (\varepsilon_S - \varepsilon_\infty) \int_{\tau_1}^{\tau_2} \frac{g(\ln\tau)d(\ln\tau)}{1 + i\omega\tau} , \qquad (2)$$

where $g(\ln\tau)$ is the distribution of relaxation times with lower and upper cutoffs τ_1 and τ_2, respectively, and normalization $\int_{\tau_1}^{\tau_2} g(\ln\tau)d(\ln\tau) = 1$. Furthermore, ε_S and ε_∞ are the usual parameters for the limiting-frequency values of the dielectric constant.

One then argues that for a sufficiently well-behaved function $g(\ln\tau)$ and for frequencies in the interval $\tau_1 \le 1/\omega \le \tau_2$, the imaginary part of the dielectric constant is essentially determined by the shape of the distribution

function,[6] i.e.,

$$\varepsilon''(\omega,T) \cong \frac{\pi}{2}(\varepsilon_S - \varepsilon_\infty) g\left(\ln\frac{1}{\omega}, T\right) . \quad (3)$$

Assuming that each inverse relaxation time $1/\tau$ obeys a relation of the type (1) with fixed ω_0, $g(\ln\tau)$ can be uniquely represented by a distribution $f(E)$ of activation energies E, i.e., $g(\ln\tau)d(\ln\tau) = f(E)dE$. Thus it follows from Eq. (3) that the data for $\varepsilon''(\omega,T)$ can be mapped in a broad frequency range onto a single curve the shape of which is determined by $f(T - T_0)$, again suggesting that T_0 should correspond to the static freezing temperature. A closer examination reveals, however, that since by assumption relation (3) is valid only in a range of frequencies ω where the relaxation spectrum $g(\ln\tau)$ varies slowly, the resulting VF scaling between the frequency and the temperature obviously excludes both cutoff regions and hence the static limit $\omega \to 0$. Thus it is not surprising that the VF mapping for DRADP has been found to break down already at frequencies below 100 Hz and above 10 MHz.[7] For the same reason, one cannot justify an analytic derivation of Eq. (1) based on the asymptotic expansion of Eq. (3) in powers of $1/\ln\omega$.

One can, of course, always try to fit the dielectric data by a suitable choice for $g(\ln\tau)$ using appropriate numerical techniques to evaluate the integral in Eq. (2). It turns out, however, that some prior knowledge about the shape of the relaxation spectrum is needed, and this information should be extracted from the data before an adequate ansatz for $g(\ln\tau)$ is written down. In a recent work,[5] it was shown that the required information about the behavior of the relaxation spectrum can readily be gained by representing the real part of the dielectric constant in the form of a so-called temperature-frequency plot. This technique should be regarded—similar to the well-known Cole-Cole plot—as a graphic representation essentially independent of the detailed shape of $g(\ln\tau)$. One can decide by mere inspection of the plots whether one of the relaxation cutoffs diverges in a given temperature range. The problem then essentially reduces to (i) the choice of a pair of suitable empirical expressions for the temperature dependences of τ_1 and τ_2, modeled according to the observed profiles of the highest and lowest curves, respectively, in the plot, and (ii) the selection of a simplest possible functional model for $g(\ln\tau)$ bearing the observed asymmetry of the spectrum. Finally, the free parameters entering these expressions can be determined by a best-fit analysis of the data. In this way, it has been shown for the case of DRADP-0.60 (Ref. 5) that the longest relaxation time τ_2 diverges according to the Vogel-Fulcher law, whereas the lower edge of the relaxation spectrum τ_1 follows a standard Arrhenius behavior.[5] Since the general expression (2) remains valid in the entire frequency range including the static limit, it is safe to identify the VF temperature T_0 with the static limit of the freezing temperature T_f. It should be noted that the basic idea relating the divergence of the longest relaxation time τ_2 to the freezing temperature is not new,[3,4,8] however, an unambiguous procedure to identify τ_2 from the data has not been described until recently,[5] and the temperature-frequency plot essentially provides the missing step.

In the present work we use the above technique to determine the freezing temperature $T_f(x)$ and hence the phase boundaries between the ergodic and nonergodic glassy phases in the (x,T) phase diagram of DRADP-x. To obtain the complete phase diagram, the analysis must be complemented by the standard procedure known from the studies of ferroelectric and antiferroelectric systems, namely, the observation of peaks and breaks, respectively, in the temperature dependences of the low-frequency dielectric constant.

Having thus determined all phase boundaries, one may try to apply the results of the static theories of dipolar glasses and test their predictions. Most theoretical considerations have so far been based on the infinite-range random-bond random-field (RBRF) Ising model,[9] which is an extension of the Sherrington-Kirkpatrick[10] (SK) model of spin glasses to proton and deuteron glasses. Formally, the link between magnetic and electric glasses is provided by assigning an Ising pseudospin to the two-state dipole moment of a proton or deuteron bond. In physical terms, however, there is an important difference between the two types of glasses, namely, the existence of local electric fields in the dipolar case, which are modeled by a set of Gaussian random fields of variance Δ in addition to the usual random interbond interactions. Random fields induce a nonzero value of the Edwards-Anderson[11] order parameter q_{EA} at all temperatures, thus smearing out the classical pseudospin glass transition.[9,12] This then creates the need for a more general definition of the freezing transition. In the static picture, the freezing line in the (T,Δ) plane separates the region above the line, where q_{EA} is a scalar quantity measuring the amount of noncooperative glassy ordering, from the true cooperative glassy phase below the line, where q_{EA} is given by the limiting value of the Parisi order parameter function $q(x)$, i.e., $q_{\mathrm{EA}} = q(1)$. By analogy with spin glasses, this line is usually referred to as the Almeida-Thouless (AT) line,[13] which can be calculated in a straightforward manner within the framework of a mean-field theory of spin glasses. The conceptual link with the previously discussed dynamic picture of a freezing transition is now established: The longest relaxation time diverges as one approaches the AT line from above, implying a transition from an ergodic pseudospin glass phase into a nonergodic one. Since in deuteron glasses the random-field variance Δ is concentration dependent, the AT line, and hence the corresponding phase boundary, becomes experimentally accessible.

Obviously, random dipolar interaction in DRADP and related systems are not infinitely ranged, thus raising some questions about the applicability of mean-field arguments to real systems. Consider, for example, the free energy of a glassy system, which is commonly described as a rugged surface in the multidimensional space of local polarizations, characterized by a set of local minima separated by high potential barriers. If the interactions are infinitely ranged, the barrier heights become infinite at the freezing temperature, and all relaxation times characterizing the transitions between these minima diverge.

In a system of finite-range interactions, however, only a fraction of these barriers are expected to become infinite, implying that only the longest relaxation time will diverge at the transition, in agreement with the dynamic picture of dielectric relaxation. Another indication of the existence of finite barriers below T_f in real systems is the fact that remanent polarization continues to decay in the frozen phase, clearly indicating that the bulk of the relaxation spectrum remains active. One may thus conclude that the static equations of the infinite-range model can only provide an approximate description of the phase boundary, and its predictions need to be tested for each particular system. So far, the static RBRF model has proven its validity in a variety of experimental studies and its application to the present problem thus seems justified.

In Sec. II of this paper we describe the experimental technique, and in Sec. III the temperature-frequency plots used in data analysis. This is followed in Sec. IV by a determination of the phase diagram based on the equations of the random-bond random-field model. Finally, in Sec. V we summarize our results.

II. EXPERIMENT

The complex dielectric constant was measured along the tetragonal a axis of DRADP-x platelets with various ammonium concentrations. Crystals of DRADP-x grown from aqueous (D_2O) solution were cut and polished to get samples having typical dimensions $5 \times 5 \times 1$ mm with planparallel surfaces normal to the tetragonal a axis. The electrodes were made using the Degussa silver paint. The concentrations of the samples were determined by chemical analysis and NMR. The temperature of the samples was stabilized and monitored to within ± 0.1 K in the temperature range from 5 K up to 300 K by an Oxford Instruments continuos flow cryostat. The dielectric constant measurements were always performed on slowly cooling (≈ 1 K/min) the system.

The complex dielectric constant was measured in the frequency range from 1 mHz to 1 MHz, which was covered by two different techniques: (a) Low-frequency measurements from 1 mHz to 1 Hz were performed via the Sawyer-Tower bridge technique. In this technique the external ac electric field is applied to the sample. The polarization charge, i.e., the corresponding voltage, was measured on a serial capacitor with known capacity by means of an electrometer. The amplitude and the phase of the voltage signal, which are proportional to the real and imaginary parts of the complex dielectric constant, respectively, were extracted by the least-squares method using a computer as a digital phase detector. (b) High-frequency measurements from 20 Hz to 1 MHz were carried out by using a HP 4284A Precision LCR meter. Both techniques complemented each other and were used successively on the samples in the ammonium concentration range $0.21 \leq x \leq 0.65$ in order to study the temperature behavior of the dielectric relaxation spectrum which in turn contains information about the critical slowing down in the glassy regime.

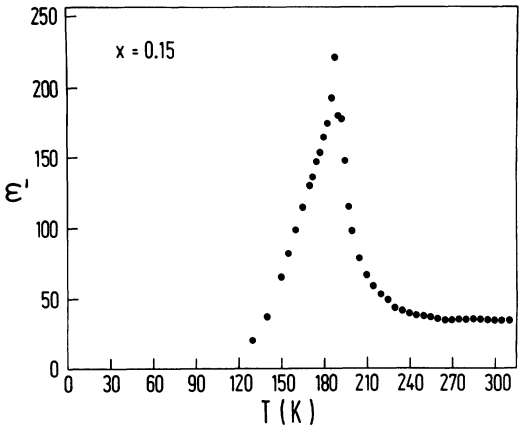

FIG. 1. Dielectric constant $\varepsilon'(\nu, T)$ at $\nu = 1$ kHz as a function of temperature in DRADP-x ($x = 0.15$).

The paraelectric-ferroelectric ($x = 0$) and paraelectric-antiferroelectric ($x = 1$) transition temperatures as well as the transitions from the ergodic glassy phase to the glassy ferroelectric phase ($x < 0.30$) and the glassy antiferroelectric phase ($x > 0.70$) were determined by measuring the peaks and breaks, respectively, in the temperature dependences of the quasistatic dielectric constant at 1 kHz. Figures 1 and 2 show ε'(1 kHz) as a function of temperature for ammonium concentrations $x = 0.15$ and $x = 0.70$. On moving away from $x = 0$ and $x = 1$ the peaks and/or breaks become more rounded and a glassy-type dielectric dispersion appears at low temperatures. The measurements at $x = 0.21$ (Fig. 3) and $x = 0.24$ (Fig. 4) in particular show the rounding of the static ε' and a shift of the frequency-dependent dielectric constant towards lower temperatures, indicating a possible coexistence of ferroelectric and glassy regions. It is interesting to note that a coexistence of an antiferrolectric behavior and a low-temperature glassy behavior is also seen on the antiferroelectric side of the phase diagram at $x = 0.70$. As shown in Fig. 5, in addition to the breaks in the dielectric constant at 115 K demonstrating the ergodic glass-antiferroelectric glass transition one finds here also a small peak in the dielectric absorption and a slight change in the shape of the temperature dependence

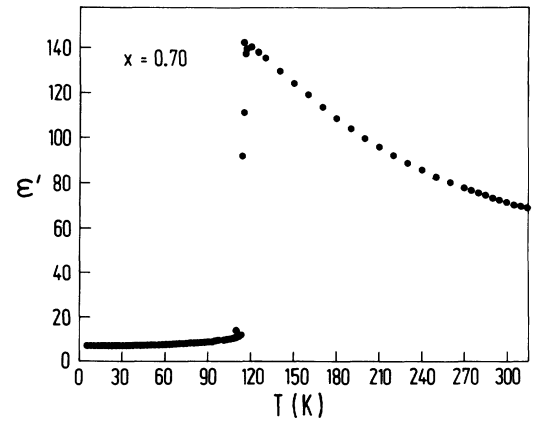

FIG. 2. Temperature dependence of $\varepsilon'(\nu, T)$ at $\nu = 1$ kHz for $x = 0.70$.

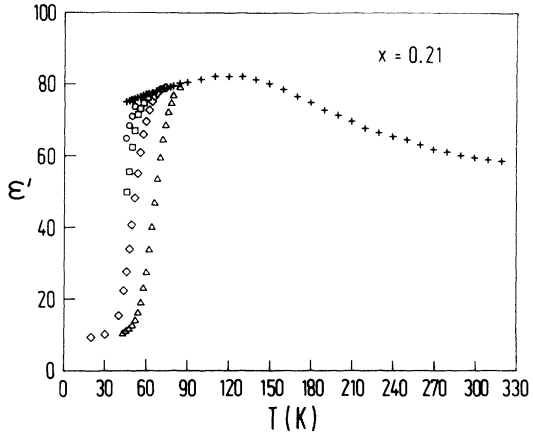

FIG. 3. Temperature dependence of the static zero-field-cooled dielectric constant ε_{ZFC} (+) for $x = 0.21$. Also shown is $\varepsilon'(\nu, T)$ at various frequencies ν: 1 MHz (△), 1 kHz (◇), 1 Hz (□), 1 mHz (○).

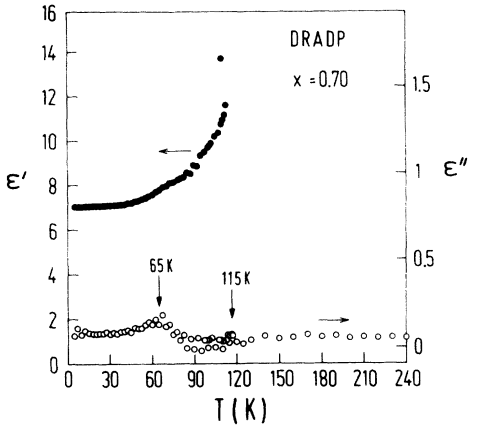

FIG. 5. Temperature dependence of ε' (•) and ε'' (○) at $\nu = 1$ kHz for $x = 0.70$.

of the real part of the dielectric constant at 65 K, indicating glassy behavior. Namely, a similar temperature behavior of the complex dielectric constant measured at 1 kHz was found in the central "glassy" region of the phase diagram.

The glassy behavior is most pronounced in the region $0.3 \leq x \leq 0.65$. Here the static dielectric constant ε_S—i.e., ε_{FC} or ε_{ZFC} in the long time limit—slowly varies with temperature and saturates as $T \to 0$ (cf. Fig. 6), while $\varepsilon^*(\nu, T)$ shows a pronounced glassy dispersion.[5] Figure 7 shows a set of typical Cole-Cole diagrams where ε'' is plotted as a function of ε' for four different temperatures, obtained on the sample with $x = 0.50$. At low temperatures the dielectric relaxation is strongly polydispersive and asymmetric, however, with increasing temperature the degree of polydispersivity is gradually diminishing and the dielectric dispersion becomes nearly monodispersive. Similar temperature behavior of the glassy dynamics was found in all measured samples with ammonium concentrations up to $x = 0.65$. Solid lines in Fig. 7 were obtained by numerical fit to a linear model for the distribution of relaxation times $g(\ln \tau)$, which will be discussed in more detail in Sec. III. The temperature dependence of the static dielectric constant ε_S obtained in this manner was independently verified by a set of zero-field-cooled polarization charge measurements, which were performed in the time domain as described previously.[14,5] It has been found that the field-cooled and zero-field-cooled static susceptibilities match on the experimental time scale t_{expt} in which the polarization charge is accumulated after switching on the electric field.

III. TEMPERATURE-FREQUENCY PLOT

The standard Cole-Cole plots described above give a clear indication that the relaxation spectrum of DRADP in the glassy regime is polydispersive and asymmetric, and furthermore its asymmetry increases strongly on lowering the temperature. In order to analyze the dielectric dispersion quantitatively one needs a specific model for the relaxation spectrum $g(\ln \tau)$ containing the above general features. As already mentioned, the choice of $g(\ln \tau)$ is greatly facilitated by introducing the temperature-

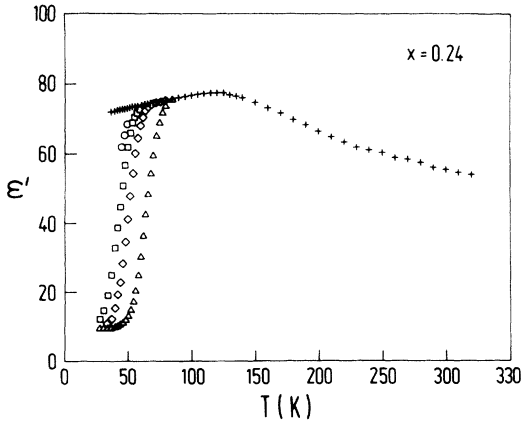

FIG. 4. Temperature dependence of the static zero-field-cooled dielectric constant ε_{ZFC} (+) for $x = 0.24$. Also shown is $\varepsilon'(\nu, T)$ at various frequencies ν: 1 MHz (△), 1 kHz (◇), 1 Hz (□), 1 mHz (○).

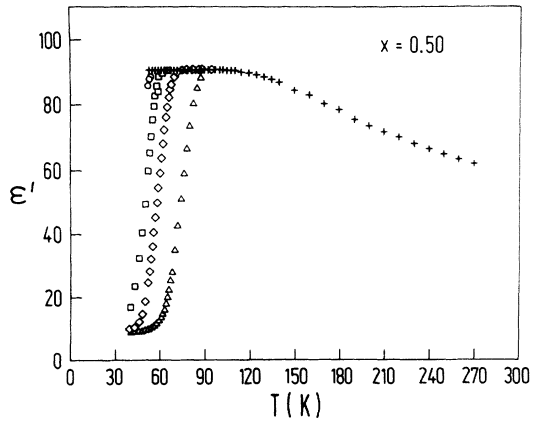

FIG. 6. Typical temperature behavior of the static zero-field-cooled dielectric constant ε_{ZFC} (+) in the glassy region, for $x = 0.50$. Also shown is $\varepsilon'(\nu, T)$ at various frequencies ν: 1 MHz (△), 1 kHz (◇), 1 Hz (□), 1 mHz (○).

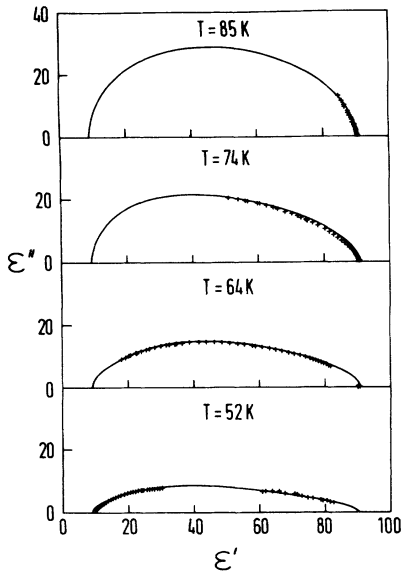

FIG. 7. Measured values of ε'' plotted vs ε' in DRADP-x ($x = 0.50$) at four temperatures, as indicated. Solid lines are fits obtained with a linear expression for the relaxation spectrum.

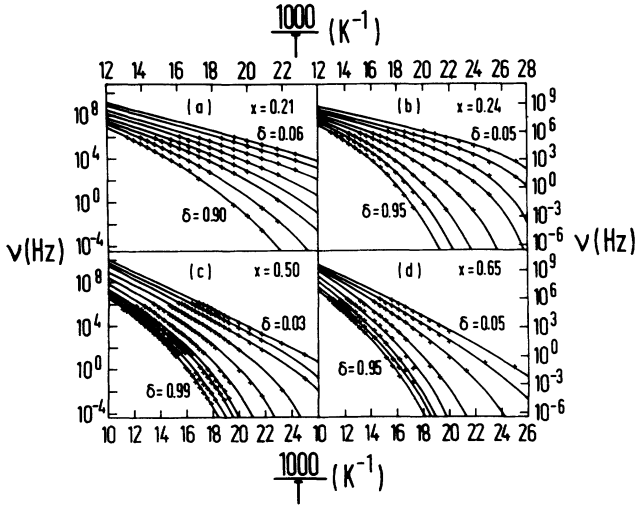

FIG. 8. Temperature-frequency plots for several fixed values of the reduced dielectric constant δ of DRADP-x at (a) $x = 0.21$, (b) $x = 0.24$, (c) $x = 0.50$, and (d) $x = 0.65$. The solid lines are calculated from Eqs. (4) and (12). The values of δ are, top to bottom, (a) 0.06, 0.10, 0.20, 0.35, 0.50, 0.65, 0.80, 0.90; (b) and (d) 0.05, 0.10, 0.20, 0.40, 0.60, 0.80, 0.90, 0.95; (c) 0.03, 0.05, 0.10, 0.25, 0.50, 0.75, 0.90, 0.95, 0.98, 0.99.

frequency plot[5] and we will here describe in some detail the essential steps of this method.

Let us therefore return to the general expression (2). Introducing a new integration variable $z = \ln(\omega_a \tau)$, where ω_a is just an arbitrary unit frequency, we can write for the real part of the dielectric constant

$$\varepsilon'(\omega) - \varepsilon_\infty = (\varepsilon_S - \varepsilon_\infty) \int_{z_1}^{z_2} \frac{g(z)dz}{1 + (\omega/\omega_a)^2 \exp(2z)} \,. \quad (4)$$

In the next step, we define a reduced dielectric constant

$$\delta = \frac{\varepsilon' - \varepsilon_\infty}{\varepsilon_S - \varepsilon_\infty} \,, \quad (5)$$

so that Eq. (4) can be symbolically rewritten as

$$\delta = I(\omega, T) \,, \quad (6)$$

where $I(\omega, T)$ represents the integral in Eq. (4). The crucial idea is now to regard δ as an experimentally adjustable parameter: By holding δ fixed at some selected value one has the possibility of investigating the behavior of $I(\omega, T)$ as a function of frequency $\nu \equiv \omega/(2\pi)$ and temperature. As one scans ε' between ε_S and ε_∞, δ will vary between the values 1 and 0. For each fixed value of δ one obtains a characteristic temperature-frequency profile in the (T, ν) plane, the set of which is referred to as the temperature-frequency or (T, ν) plot. Some typical (T, ν) plots for samples with various concentrations x are shown in Fig. 8. Since the value of $I(\omega, T)$ is determined solely by the relaxation spectrum $g(z)$ including its cutoffs z_1 and z_2, the (T, ν) plots are expected to provide insight into the temperature variation of the various segments of $g(z)$.

To see that more clearly, let us examine qualitatively the behavior of the integral $I(\omega, T)$. The steplike filter represented by the factor $1/\left[1 + (\omega/\omega_a)^2 \exp(2z)\right]$ in the integral in Eq. (4) effectively suppresses the contributions due to values of z larger than $z_{\max}(\omega) = \ln(\omega_a/\omega)$. Thus the value of the integral is approximately

$$I(\omega, T) \approx \int_{z_1}^{\ln(\omega_a/\omega)} g(z)dz \,. \quad (7)$$

Clearly, for small values of δ only the part of $g(z)$ near z_1 will contribute, and thus the filter will probe the shape of the relaxation spectrum near its lower cutoff. In particular, the temperature dependence of $I(\omega, T)$ will be mainly determined by the behavior of $z_1(T)$. On the other hand, for δ close to 1, the filter will scan the function $g(z)$ near its upper cutoff, and $I(\omega, T)$ will mirror the temperature behavior of $z_2(T)$.

The point we wish to emphasize here is that the above qualitative conclusions remain applicable if instead of the approximate relation (7) one considers the exact value of $I(\omega, T)$. The latter can, of course, be gained by evaluating the integral in Eq. (4) numerically with a trial function $g(z)$. Therefore, a mere inspection of the plot—before any calculated curves have been drawn—should provide a reliable qualitative description of the temperature variation of the relaxation cutoffs $z_1(T)$ and $z_2(T)$. For example, in the plots presented in Fig. 8 the data corresponding to the smallest value of δ appear to be lying nearly on a straight line, suggesting a linear relationship between z_1 and $1/T$ of the type

$$z_1(T) = z_{10} + E/T \,. \quad (8)$$

This, in turn, implies an Arrhenius-type behavior of the shortest relaxation time, namely,

$$\tau_1 = \tau_{10} \exp(E/T) \,. \quad (9)$$

In contrast, the lowest curves for δ close to 1 fall off dramatically as the temperature is lowered, indicating a possible divergent behavior of $z_2(T)$. An appropriate ansatz should therefore be written as

$$z_2(T) = z_{20} + U/(T - T_0)^{\beta} , \tag{10}$$

leading for $\beta = 1$ to a Vogel-Fulcher behavior of τ_2, i.e.,

$$\tau_2 = \tau_{20} \exp[U/(T - T_0)] . \tag{11}$$

The parameters τ_{10}, τ_{20}, E, U, T_0, and β are to be determined by a best-fit analysis of the data based on the exact numerical evaluation of $I(\omega, T)$. For DRADP the best fit at all concentrations was obtained with the following asymmetric linear ansatz for $g(z)$:

$$g(z) = 2\frac{z_2 - z}{(z_2 - z_1)^2} , \quad z_1 \leq z \leq z_2 , \tag{12}$$

which does not contain any additional parameters. The solid lines in Fig. 8 were obtained by fitting $I(\omega, T)$ evaluated numerically for the above function $g(z)$ to the (T, ν) plots. It turns out that $\beta \approx 1$ in all the cases investigated. The values of the remaining parameters are summarized in Table I.

The same linear model (12) has been used to draw the solid lines appearing in the Cole-Cole plots in Fig. 7 and has in general produced very good results, in particular in the low-frequency range. In the present analysis we have explicitly focused on the upper, i.e., long time part of the relaxation spectrum, which shows divergent behavior and hence contains information about the freezing process.

It should again be stressed that the (T, ν) plots were introduced in order to obtain a qualitative description of the asymmetric behavior of the relaxation spectrum, including its cutoffs. The essential information supplied by these plots is that only the upper cutoff scales according to the VF law, not each part of the relaxation spectrum, as already pointed out in the Introduction following Eq. (3). In fact, one can show that if in evaluating $I(\omega, T)$ one assumes a VF scaling of each relaxation time in the spectrum, the resulting (T, ν) profiles will all diverge at the same temperature T_0, in obvious disagreement with the data. Since $\tau_{\max} = \tau_2$ diverges as $T \to T_0$, the present method clearly suggests that the fit parameter T_0 corresponds to the static or equilibrium value of the freezing temperature $T_f(t_{\text{expt}} \to \infty)$, which would in principle be observable on an infinite time scale only.

Finally, we note that in any actual experiment one cannot measure the dielectric dispersion at a fixed value of ε'—and hence of δ—which may seem to be required in order to generate the (T, ν) plot. A practical solution is to group the raw data around a set of suitable values of δ and then use a standard numerical interpolation procedure to obtain the corresponding fixed δ points.

TABLE I. Fit parameters as functions of ammonium concentration x.

x	T_0 (K)	τ_{10} (10^{-15} s)	U (K)	τ_{20} (10^{-12} s)	E (K)
0.21	27.5 ± 2	6.3 ± 4.0	850 ± 100	2.4 ± 1.2	940 ± 150
0.24	31.4 ± 1	5.9 ± 3.5	760 ± 100	5.0 ± 5.0	800 ± 150
0.50	32.9 ± 1	3.7 ± 1.4	780 ± 100	3.0 ± 1.8	1060 ± 150
0.60	32.9 ± 0.5	5.6 ± 1.8	770 ± 70	1.8 ± 0.7	980 ± 70
0.65	31.7 ± 1	3.2 ± 1.0	950 ± 100	2.8 ± 1.6	1100 ± 150

IV. PHASE DIAGRAM OF DRADP

The phase diagram of DRADP-x obtained by the method outlined in Secs. II and III is shown in Fig. 9. The squares represent the transition temperatures determined from the peaks and breaks in $\varepsilon'(T)$, the open circles the VF temperatures T_0, and the solid circles the transition temperatures determined by NMR.[15] It is interesting to note that the freezing temperature $T_0(x)$ is nearly independent of the ammonium concentration x in the entire glassy regime $0.3 \leq x \leq 0.65$ where we find $T_0 = 33 \pm 0.5$ K.

The solid lines in Fig. 9 have been calculated from the static random-bond random-field model of deuteron glasses. As already pointed out in the Introduction, a mean-field theory based on the infinite-ranged RBRF model can only provide an approximate description of the freezing transition in a system with finite-range interactions. In the present problem, we want to address the crucial question whether the freezing line $T_0 = T_0(x)$ could be interpreted as the Almeida-Thouless (AT) line separating the ergodic glassy phase from the nonergodic one in the temperature random-field variance (Δ, T) plane. Namely, the $T_0 = T_0(x)$ line can be related to the AT line $T_f = T_f(\Delta)$, as a variation in the ammonium concentration x induces a variation in the random-field variance Δ. Thus we assume that the $T_0 = T_0(x)$ line is

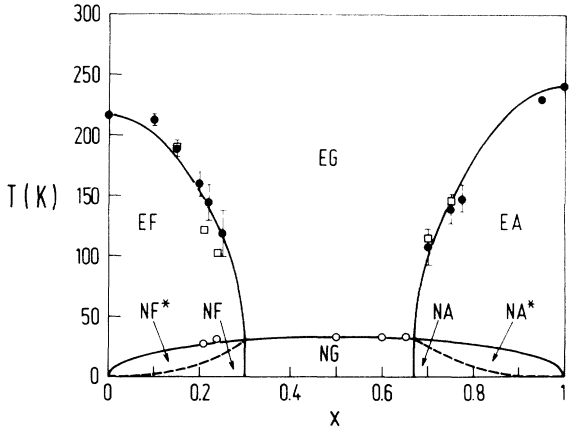

FIG. 9. Phase diagram of DRADP-x system exhibiting the various phases, labeled as E (ergodic), N (nonergodic), G (glass), F (ferroelectric, $P \neq 0$), F^* (ferroelectric, $P = 0$), A (antiferroelectric, $P \neq 0$), A^* (antiferroelectric, $P = 0$). □, transition temperatures determined from the peaks and/or breaks in $\varepsilon'(T)$; ○, Vogel-Fulcher temperature T_0 obtained from the divergence of $\tau_{\max}$; •, transition temperatures measured by NMR (Ref. 15). Solid lines are calculated from the static RBRF model.

describable by the static RBRF model

$$H = -\frac{1}{2}\sum_{ij} J_{ij} S_i S_j - \sum_i f_i S_i \,, \tag{13}$$

where the pseudospin $S_i = \pm 1$ refers to the two equilibrium deuteron positions in the ith O − D ··· O bond. The random bonds are assumed to have a Gaussian probability distribution with a mean J_0/N and variance J^2/N, while the random fields f_i are distributed according to an independent Gaussian distribution with mean zero and variance Δ. Formally the phase boundary $T_f(x)$ which separates the ergodic glassy phase from the nonergodic one—i.e., the AT line—is obtained from the coupled self-consistent equations which determine the values of the spin glass order parameter q and the single-domain polarization P in the ferroelectric case, or the sublattice polarization P in the antiferroelectric case, and the stability condition for the replica symmetric solution. For the case $J_0 = 0$ (i.e., $P = 0$) these equations are explicitly given in Ref. 9 and can easily be generalized to the more general case discussed here, $J_0 = J_0(x) \neq 0$. To facilitate further discussion and possible applications to related systems we write down these generalized equations:

$$q = \int_{-\infty}^{+\infty} Dz \tanh^2 [h_z(x)/T_f(x)] \,, \tag{14}$$

$$P = \int_{-\infty}^{+\infty} Dz \tanh [h_z(x)/T_f(x)] \,, \tag{15}$$

$$[T_f(x)/J(x)]^2 = \int_{-\infty}^{+\infty} Dz \cosh^{-4} [h_z(x)/T_f(x)] \,, \tag{16}$$

where $Dz \equiv dz \exp(-z^2/2)$ and $h_z(x) \equiv J(x) z \sqrt{q + \tilde{\Delta}} + |J_0(x)| P$. We may assume, as usual, that $J(x) = J_{\max}\sqrt{x(1-x)}$ and $\Delta = \Delta_{\max}\sqrt{x(1-x)}$, so that $\tilde{\Delta} \equiv \Delta/J^2$ is independenent of the concentration x.

The phase boundaries which separate the ergodic glass from the ergodic ferroelectric and antiferroelectric glassy phases are obtained for $|J_0(x)| \geq J(x)$ from the condition for the divergence of the corresponding susceptibilities,

$$T_C(x) = J_0(x)\{1 - q[T_C(x)]\} \,, \tag{17}$$

together with Eq. (14) for $q(T_C)$ with $P = 0$. Here $P = 0$ since the spontaneous polarization vanishes at each of these boundaries. It is interesting to note that the observed ferroelectric and antiferroelectric phase boundaries cannot be described by the usual linear concentration dependence of $J_0(x)$, which is appropriate for "linear" solid solutions, but require in the case of DRADP-x a cubic polynomial of the following form:[7]

$$J_0(x) = (1-x)T_{\rm FE} - xT_{\rm AFE} - 2x(1-x)\left\{(T_{\rm FE} - T_{\rm AFE})/2 - \left[(1-x)T_{\rm FE}^{AB} - xT_{\rm AFE}^{AB}\right]\right\} \,. \tag{18}$$

An expression of this general type can be derived by considering all relevant pairwise interactions among deuteron bonds in a solid solution of two constituents A and B. The parameters $T_{\rm FE}$ and $T_{\rm AFE}$ correspond to the ferroelectric and antiferroelectric critical temperature T_C, respectively, for the two pure cases $x = 0$ (C = FE) and $x = 1$ (C = AFE). These are independently known from earlier experiments, i.e., $T_{\rm FE} = 217$ K and $T_{\rm AFE} = 242$ K.[15] The values of the remaining two parameters $T_{\rm FE}^{AB}$ and $T_{\rm AFE}^{AB}$ will be determined from the phase diagram, as described below.

For $J(x) > |J_0(x)|$, P is identically zero and the AT line separates the ergodic glass phase from the nonergodic glass phase. This line is practically independent of the ammonium concentration x as indeed observed (Fig. 9) in the interval $0.3 \leq x \leq 0.65$. For $J(x) < |J_0(x)|$, on the other hand, the polarization P on the ferroelectric side and the sublattice polarization P on the antiferroelectric side are nonzero for a single-domain state. The AT line which separates here the ergodic ferroelectric and ergodic antiferroelectric glassy phases from the corresponding nonergodic ones is concentration dependent. For $J(x) < |J_0(x)|$, on the other hand, one would expect according to the usual mean-field arguments that P is nonzero and should be given by the solution of Eq. (15). However, it is well known that a single-domain state cannot be sustained in a random-field system which has been cooled from the unpolarized high temperature phase. Rather, the system may break up into microdomains of opposite orientations[16] implying that effectively $P = 0$. Thus the stability limit of the ergodic spin glass phase within the "ferroelectric" region can be estimated by extrapolating the AT line for $P = 0$ into the region $x < 0.3$. This is shown as a solid line in Fig. 9. Also indicated is the single-domain stability limit formally obtained by the solution of Eqs. (14)–(16). The two experimental points at $x = 0.21$ and $x = 0.24$ agree rather well with the predicted $P = 0$ freezing line. An alternative picture would be that a phase segregation between "ferroelectric" and "glassy" regions occurs for $0.2 < x < 0.3$, as suggested by ^{87}Rb NMR measurements,[15] again implying that $P = 0$ at the freezing transition. At present we cannot decide which of the above arguments—or perhaps a combination of both—is applicable to the system under study. In each case, however, the AT line has to be calculated at $P = 0$ as in fact borne out by the experimental data. Further experiments, including a search for spontaneous polarization at various concentrations, are needed in order to discriminate between the above possibilities. On the antiferroelectric side, the AT line is unobservable by dielectric spectroscopy as the critical dispersion occurs at the Brillouin zone boundary rather than the zone center. It should be noted that Takashige *et al.*[17] were the first to observe the coexistence of antiferroelectric and glassy phases on an undeuterated DRADP-x sample with $x = 0.75$, which they attributed to reentrant behavior.

The phase boundaries between the nonergodic ferroelectric and/or antiferroelectric glassy regions with $P = 0$ and the nonergodic glassy region where $P = 0$ have been derived from Eq. (17) with q being replaced by the Parisi one-step approximation for the order parameter function.[18] All phase boundaries in the phase diagram in Fig. 9 have been thus obtained from the static RBRF model with the following set of parameters: $\tilde{\Delta} = 0.93 \pm 0.05$, $J_{\max} = 164.8 \pm 5$ K, $T_{\mathrm{AFE}}^{AB} = 290 \pm 10$ K, and $T_{\mathrm{FE}}^{AB} = 270 \pm 10$ K. It is particularly interesting that the experimentally determined points on the freezing transition line $T_0 = T_0(x)$ perfectly agree with the AT line evaluated from the static RBRF model.

V. SUMMARY

The frequency-dependent complex dielectric constant of the deuteron glass $Rb_{1-x}(ND_4)_xD_2PO_4$ (or DRADP-x) has been measured and analyzed as a function of temperature and ammonium concentration x. A recently introduced technique based on the temperature-frequency or (T, ν) plots indicates that in the glassy regime the maximum relaxation time diverges according to the Vogel-Fulcher (VF) law. The corresponding VF temperature T_0 has been identified as the static limit of the freezing temperature T_f, thus yielding the freezing line in the (x, T) phase diagram of DRADP-x.

The results have been analyzed in terms of the static random-bond random-field (RBRF) model of dipolar glasses. According to this model, the freezing line $T_0 = T_0(x)$ corresponds to the Almeida-Thouless (AT) line $T_f = T_f(\Delta)$ in the temperature random-field variance (T, Δ) plane separating the ergodic pseudospin glass phase from the nonergodic one. The phase diagram of DRADP-x in the entire range of concentration x has been calculated from the equations of the static RBRF model including the x-dependent mean value of the random-bond distribution $J_0(x)$. It follows that all boundaries can be well described by the RBRF model if one takes into account the nonlinear character of $J_0(x)$. The phase boundary between the ergodic and nonergodic glass phases of DRADP-x thus obtained shows a rather weak x dependence. The boundaries of the ergodic ferroelectric and antiferroelectric phases agree well with earlier results obtained by NMR experiments. It should be noted that it has been widely held so far—particularly in the case of magnetic spin glasses—that the AT line cannot be determined experimentally in view of the extremely long relaxation times occurring on approaching the freezing transition. The present work explicitly demonstrates that the static limit can be made accessible by a suitable extrapolation of the temperature dependence of the maximum relaxation time.

The observed glassy dynamics within the ferroelectric region suggests the absence of macroscopic polarization for concentrations $0.2 < x < 0.3$. This is tentatively interpreted as being due to the formation of microdomains in the presence of random local fields. Alternatively, a phase segregation between nanosized "ferroelectric" and "glassy" regions may be occurring, again implying the suppression of long-range ferroelectric order in this concentration range. Further experiments including a search for spontaneous polarization are required.

ACKNOWLEDGMENTS

This work was supported by the Ministry of Research and Technology of the Republic of Slovenia and the Commission of the European Communities.

* Present address: Department of Chemistry and Center for Materials Science and Engineering, Massachusetts Institute of Technology, Cambridge, Massachusetts 02139.

[1] E. Courtens, J. Phys. (Paris) Lett. **43**, L199 (1982); Ferroelectrics **72**, 229 (1987).
[2] U.T. Höchli, K. Knorr, and A. Loidl, Adv. Phys. **39**, 405 (1990).
[3] R.G. Palmer, D.L. Stein, E. Abrahams, and P.W. Anderson, Phys. Rev. Lett. **53**, 958 (1984).
[4] M.V. Feigel'man and L.B. Ioffe, J. Phys. (Paris) Lett. **46**, L695 (1985).
[5] Z. Kutnjak, C. Filipič, A. Levstik, and R. Pirc, Phys. Rev. Lett. **70**, 4015 (1993).
[6] E. Courtens, Phys. Rev. B **33**, 2975 (1986).
[7] Z. Kutnjak, Ph.D. thesis, University of Ljubljana, 1994.
[8] F. Wickenhöfer, W. Kleemann, and D. Rytz, Ferroelectrics **124**, 273 (1991); **135**, 333 (1992).
[9] R. Pirc, B. Tadić, and R. Blinc, Phys. Rev. B **36**, 8607 (1987).
[10] D. Sherrington and S. Kirkpatrick, Phys. Rev. Lett. **35**, 1792 (1975).
[11] S.F. Edwards and P.W. Anderson, J. Phys. F **5**, 965 (1975).
[12] R. Blinc, J. Dolinšek, R. Pirc, B. Tadić, B. Zalar, R. Kind, and O. Liechti, Phys. Rev. Lett. **63**, 2248 (1989); see also S. Chen, D.C. Ailion, and G. Laicher, Phys. Rev. B **47**, 3047 (1993).
[13] J.R.L. de Almeida and D.J. Thouless, J. Phys. A **11**, 983 (1987).
[14] A. Levstik, C. Filipič, Z. Kutnjak, I. Levstik, R. Pirc, B. Tadić, and R. Blinc, Phys. Rev. Lett. **66**, 2368 (1991).
[15] N. Korner, Ch. Pfammatter, and R. Kind, Phys. Rev. Lett. **70**, 1283 (1993).
[16] J. Villain, Phys. Rev. Lett. **52**, 1543 (1984).
[17] M. Takashige, H. Terauchi, Y. Miura, and S. Hoshino, J. Phys. Soc. Jpn. **54**, 3250 (1985).
[18] G. Parisi, Phys. Lett. **73A**, 203 (1979); J. Phys. A **13**, 1101 (1980).